

Scattering-layer-induced energy storage function in polymer-based quasi-solid-state dye-sensitized solar cells

Xi Zhang and Hongrui Jiang

Citation: [Applied Physics Letters](#) **106**, 103903 (2015); doi: 10.1063/1.4914585

View online: <http://dx.doi.org/10.1063/1.4914585>

View Table of Contents: <http://scitation.aip.org/content/aip/journal/apl/106/10?ver=pdfcov>

Published by the [AIP Publishing](#)

Articles you may be interested in

[Enhanced conversion efficiency of dye-sensitized solar cells using a CNT-incorporated TiO₂ slurry-based photoanode](#)

[AIP Advances](#) **5**, 027118 (2015); 10.1063/1.4908179

[Application of 3A molecular sieve layer in dye-sensitized solar cells](#)

[Appl. Phys. Lett.](#) **105**, 083907 (2014); 10.1063/1.4894183

[Carbon nanotube based flexible counter electrode for quasi-solid state dye sensitized solar cells](#)

[J. Renewable Sustainable Energy](#) **6**, 043116 (2014); 10.1063/1.4892546

[MgO-hybridized TiO₂ interfacial layers assisting efficiency enhancement of solid-state dye-sensitized solar cells](#)

[Appl. Phys. Lett.](#) **104**, 063303 (2014); 10.1063/1.4864319

[Ti O₂ single-crystalline nanorod electrode for quasi-solid-state dye-sensitized solar cells](#)

[Appl. Phys. Lett.](#) **87**, 113113 (2005); 10.1063/1.2048816

A promotional banner for COMSOL 5.0. It features a background of colorful, flowing lines in shades of blue, green, yellow, and red, set against a light gray grid. The text 'Build and Run Simulation Apps with COMSOL 5.0' is prominently displayed in a dark red font. Below the text is a dark red button with a white play icon and the text 'SEE HOW'. The COMSOL logo is in the bottom right corner.

Scattering-layer-induced energy storage function in polymer-based quasi-solid-state dye-sensitized solar cells

Xi Zhang and Hongrui Jiang^{a)}

Materials Science Program, Department of Electrical and Computer Engineering,
University of Wisconsin-Madison, Madison, Wisconsin 53706, USA

(Received 11 February 2015; accepted 1 March 2015; published online 11 March 2015)

Photo-self-charging cells (PSCs) are compact devices with dual functions of photoelectric conversion and energy storage. By introducing a scattering layer in polymer-based quasi-solid-state dye-sensitized solar cells, two-electrode PSCs with highly compact structure were obtained. The charge storage function stems from the formed ion channel network in the scattering layer/polymer electrolyte system. Both the photoelectric conversion and the energy storage functions are integrated in only the photoelectrode of such PSCs. This design of PSC could continuously output power as a solar cell with considerable efficiency after being photo-charged. Such PSCs could be applied in highly-compact mini power devices. © 2015 AIP Publishing LLC.
[<http://dx.doi.org/10.1063/1.4914585>]

Hybridization of photoelectric conversion and energy storage functions in devices has attracted great attentions in recent years due to the increasing demand of renewable energy around the world and the miniaturization and multi-functionalization in electronics industry.^{1–13} Typically, such photo-self-charging cells (PSCs) consist of two independent sections, a solar cell and a supercapacitor/lithium ion battery. Thus, there were three electrodes in these PSCs.^{1–7} Another type of PSCs could be regarded as simplex devices, since they contain only two electrodes: One is for solar energy conversion (photoelectrode) and the other is for energy storage (counter electrode, CE).^{8–13} Traditional two-electrode PSCs could not provide continuous power output after being fully charged under steady illumination, since the photo-generated charges are depleted to charge the energy storage section.^{8–10} In our previous work, a new type of two-electrode PSC based on dye-sensitized solar cells (DSSCs) was reported with both good photo-to-electric conversion efficiency (η) and energy storage capacity via introducing composited ZnO/polyvinylidene fluoride (PVDF) nanostructure in CE.¹² The polymer/nanostructured oxide system could possess energy storage capability while allowing the passage of carriers through the structure. The energy storage performance of PSCs depends heavily on the functionalization of CEs. So far, all PSCs rely on functionalized CEs for energy storage. In this study, we realized even more compact two-electrode PSCs by integrating both the solar energy conversion and the energy storage functions to the photoelectrode. Polymer-based DSSCs are one kind of popular quasi-solid-state DSSCs owing to their excellent characteristics such as easy fabrication, low cost, good stability, and flexibility.^{14–20} Although scattering layer is not usually applied in such cells due to the reduction of electron transport, our findings show that adding a scattering layer of large TiO₂ nanoparticles in a polymer-based quasi-solid-state DSSCs could form scattering layer/polymer matrix structure

for energy storage. There was no additional structure for energy storage on the CE of such PSC. Experimental results showed that such PSC could operate as a solar cell under illumination, while some of the charges are stored. After the light source was removed, the stored charges could be outputted in current. We proved that the scattering layer/polymer electrolyte in connection with the TiO₂ active layer plays the role of storing charges when the light source is turned off.

As shown in Fig. 1(a), three cells were fabricated in this study (C1, C2, and C3). Each of the cells consisted of three components: a photoelectrode, a CE, and electrolyte. For the photoelectrode, 8- μ m-thick TiO₂ photoactive layer was deposited onto a conductive fluorine-doped tin oxide (FTO) glass substrate using a screen printing method²¹ with a paste composed of 15–20 nm TiO₂ particles, before sintering at 500 °C for 1 h. The area of the active region on the FTO glass was 0.12 cm². In the two cells C1 and C2, a 2- μ m-thick TiO₂ scattering layer composed of 50–100 nm TiO₂ particles was deposited on top of the TiO₂ photoactive layer, followed by sintering at 500 °C for 1 h. After being dipped into 0.05 M TiCl₄ aqueous solution at 70 °C for 30 min, all three photoelectrodes were sintered at 450 °C for 30 min before being cooled down to 120 °C and soaked into the dye solution [0.3 mM N719 in acetonitrile/tertbutanol, v:v = 1:1] for 24 h. The CEs in the three cells were the same: Pt-coated FTO with two drilled holes for injection of the electrolyte. The photoelectrode of C2 was dip-coated with a quasi-solid-state electrolyte [0.1 M LiI, 0.05 M I₂, 0.6 M 1,2-dimethyl-3-propylimidazolium iodide, and 2 wt. % poly(vinylidene fluoride-co-hexafluoropropylene) (PVDF-HFP) (M_w = 455,000) in acetonitrile/dimethyl sulfoxide (v:v = 4:1)], before being dried on a hot plate at 40 °C for 10 min. All three photoelectrodes were sealed with CEs, respectively, using 25- μ m-thick surlyn as spacers. After this step, C1 and C3 were filled with the same quasi-solid-state electrolyte as above. The electrolyte solution was repeatedly injected into the space between the photoelectrodes and the CEs and dried on the hot plate at 40 °C until the porous nano-TiO₂ was fully filled

^{a)}Author to whom correspondence should be addressed. Electronic mail: hongrui@engr.wisc.edu. Tel.: 1-608-265-9418.

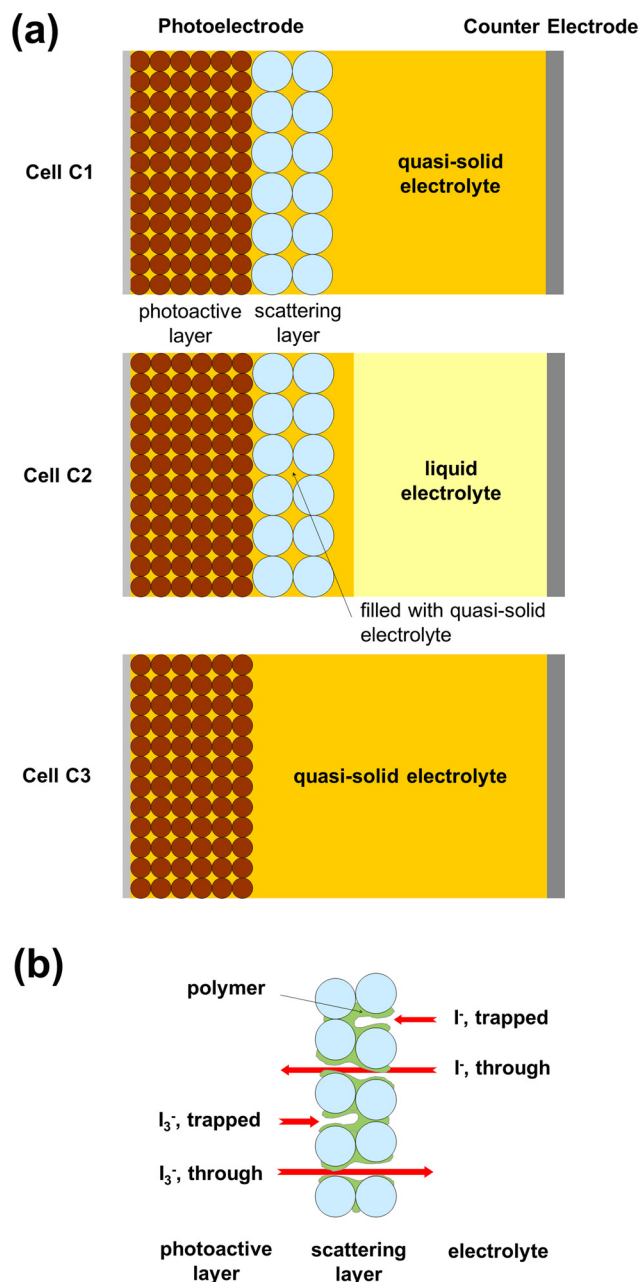


FIG. 1. (a) Schemes of the device structure of the three types of cells in this study. Cell C1 contains scattering layer and quasi-solid electrolyte; cell C2 contains quasi-solid electrolyte filled scattering layer and liquid electrolyte; cell C3 contains quasi-solid-state electrolyte but no scattering layer. (b) Charging process in the polymer electrolyte/scattering layer: part of I_3^- and I^- ions are trapped while the other I_3^- and I^- ions transport through the scattering layer for photo-to-electric conversion.

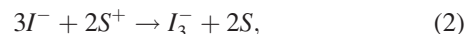
and the solvent was sufficiently removed, before the holes in the CEs were finally sealed. For C2, a liquid electrolyte [0.1 M LiI, 0.05 M I_2 , and 0.6 M 1,2-dimethyl-3-propylimidazolium iodide in acetonitrile] was filled before the holes in the CE were sealed.

The polymer electrolyte filled the spaces in the scattering layer, which was formed by larger TiO_2 particles. As is well known, the polymer could form a matrix in the quasi-solid electrolyte to provide the transport paths for ions.^{22,23} The contact between the polymer matrix and the surface of the large TiO_2 nanoparticles in the pores of the scattering layer could form some cavities to hold I^- ions for energy

storage. When a DSSC is illuminated, the I_3^- ions are converted to I^- ions at the CE via the reaction



The generated I^- ions at the CE then diffuse towards the photoelectrode through the electrolyte. Meanwhile, the I^- ions are converted back to I_3^- ions to provide electrons to the oxidized dyes (S^+) in the photoactive layer region via the reaction



where S is the regenerated ground state of the dyes. The generated I_3^- ions then diffuse towards the CE through the electrolyte. When the ions reach the steady state, the distributions of I_3^- and I^- along the cell are: the I_3^- ions are concentrated in the photoactive layer region, while the I^- ions are concentrated in the electrolyte region. In a PSC, while most of the I_3^- and I^- ions transport through the polymer electrolyte/scattering layer in the two opposite directions, some of them could be adsorbed and trapped in the matrix structure, as shown in Fig. 1(b). The adsorbed I_3^- ions could not reach the pure electrolyte region while the adsorbed I^- ions could not reach the photoactive layer region. However, the ion distribution states are almost the same as those in a DSSC with light on. After the light is turned off, each of the I_3^- and I^- concentrations in DSSC reaches an equilibrium state across all the regions via the recombination process. On the contrary, in the PSC, the adsorbed I_3^- and I^- in the scattering layer region maintain their respective distributions even after the light is turned off. When the PSC is short-circuited, the I^- ion concentration difference between the photoactive layer region and the pure electrolyte region could force I^- to diffuse towards the CE and to be oxidized back to I_3^- ,



The generated electrons could then transport through the external circuit to the photoelectrode. This is the main mechanism of the charging and discharging of the polymer electrolyte/scattering layer and the reversal of the current after the light is turned off. An important criterion for the adsorbed ions to realize the energy storage function is that the recombination paths from I^- to dye/ TiO_2 are blocked via the polymer matrix.

The transient curves of charging-discharging current and discharging voltage ($V-t$, $J-t$) of the cells were measured by an Agilent 34411 A 61/2 digital multimeter, and the results are plotted in Figs. 2(a) and 2(b). The cells were illuminated under AM 1.5 G for 2 minutes before the light was shut down for discharging: in short-circuit for $J-t$, and through a 1 M Ω resistor for $V-t$. After photo-charging, each of the discharging curves of C1 and C2 showed a reversed direction of current, indicating a charging-discharging process occurring. For C3, the current rapidly dropped to zero without reversal after the light was shut down. This pure quasi-solid-state DSSC without scattering layer thus did not show any energy storage function because only forward recombination current was observed. Therefore, the scattering layer in the quasi-solid

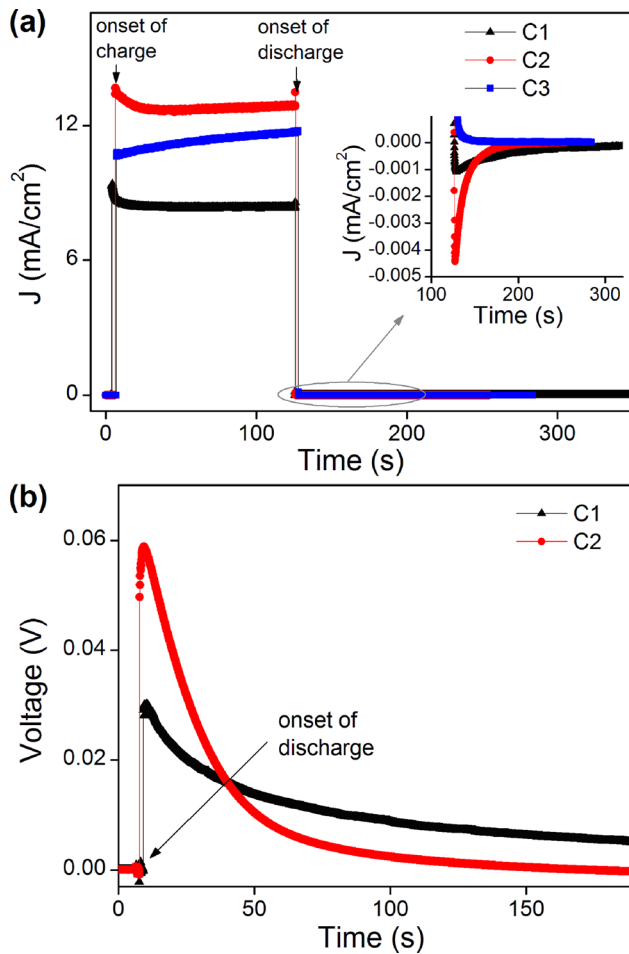


FIG. 2. (a) J - t curves of C1, C2, and C3, discharged in short circuit. The inset: discharge curves zoomed in. (b) V - t curves of C1 and C2, discharged through a 1 MΩ resistor. For both the J - t and V - t curves, the cells were illuminated under AM 1.5G for 2 min before the light was shut down for discharging.

electrolyte played an important role for the energy storage. Fig. 2(b) shows the discharging voltage transient curves of C1 and C2. For each of these two cells, the voltage polarity was reversed with respect to the photovoltage when the discharging began, indicating that the discharging voltage came from the photo-charged section. As shown in Fig. 1(a), the

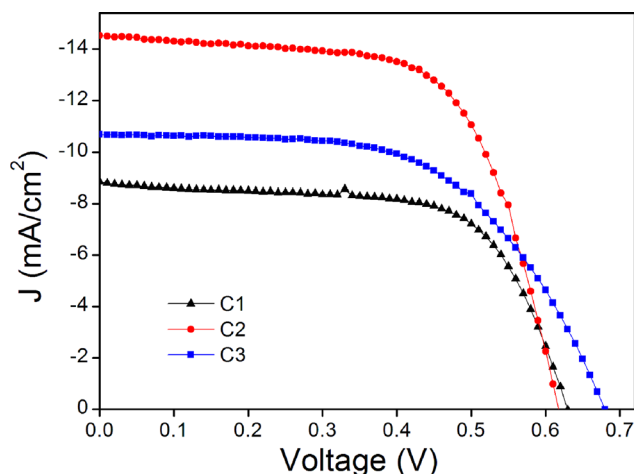


FIG. 3. J - V curves of C1, C2, and C3 under AM 1.5 G.

TABLE I. Performance parameters of the three cells.

Samples	V_{oc} (V)	J_{sc} (mA cm ⁻²)	FF	η (%)	Stored charge density (C g ⁻¹)
C1	0.63	8.84	0.653	3.64	0.653
C2	0.62	14.5	0.642	5.78	0.442
C3	0.69	11.0	0.553	4.19	...

photoelectrode of C2 was filled with quasi-solid electrolyte, and the space between the photoelectrode and the CE was filled with liquid electrolyte. Hence, this CE did not contribute to any energy storage since there was no polymer in contact with CE. This result further proves the energy storage ability of the scattering layer in quasi-solid-state electrolyte. In the scattering layer, the pure energy storage material is the dielectric polymer matrix in the pores formed by the large TiO₂ particles.^{12,13} The charge-storage densities of C1 and C2 were calculated to be 0.653 C g⁻¹ and 0.442 C g⁻¹, respectively, by integration of their reverse J - t curves over the mass of the polymer electrolyte in the scattering layer. The energy storage level of the two cells is comparable with that of previously reported two-electrode PSCs which were based on ZnO/PVDF nanostructure in CE.¹²

The photocurrent density-voltage (J - V) curves of the three cells were measured under AM 1.5G simulated solar illumination after they were sufficiently illuminated, and the results are shown in Fig. 3. All the J - V parameters are shown in Table I. The PSCs C1 and C2 still kept a high photo-to-electric conversion performance after they were charged. Because of the matrix network of ion paths formed by the polymer, the operations of photo-to-electric conversion and charge storage could proceed separately with limited interaction. The performance of C2 is even greater than the pure solar cell C3, since the main component of the electrolyte in C2 is liquid. Comparing with traditional quasi-solid-state DSSC C3, the V_{oc} of PSCs C1 and C2 is reduced due to the stored charges. C1 shows both considerable η of 3.64% and energy storage capacity of 0.653 C g⁻¹.

In conclusion, we realized two-electrode PSCs with highly compact structure based on quasi-solid-state DSSCs and energy-storage-functionalized scattering layer/polymer electrolyte. Both the photoelectric conversion and the energy storage functions could be integrated in the photoelectrode. By replacing the quasi-solid electrolyte between the scattering layer and the CE with liquid electrolyte, it was proved that the energy storage function came from the scattering layer/polymer electrolyte structure. This device possessed both considerable η of 3.64% and charge storage density of 0.653 C g⁻¹. Such PSCs with highly-compact structure could play a key role in mini electronic devices with multiple functions. In our future work, energy storage capacity could be improved by optimizing the thickness and structure of the scattering layer, and exploring new types of electrolyte.

This work was supported by the U.S. National Institutes of Health (Grant No. 1DP2OD008678). This research utilized NSF supported shared facilities at the University of Wisconsin. The authors thank Dr. X. Huang for technical assistance and discussion.

- ¹T. N. Murakami, N. Kawashima, and T. Miyasaka, *Chem. Commun.* **2005**, 3346.
- ²H.-W. Chen, C.-Y. Hsu, J.-G. Chen, K.-M. Lee, C.-C. Wang, K.-C. Huang, and K.-C. Ho, *J. Power Sources* **195**, 6225 (2010).
- ³G. Wee, T. Salim, Y. M. Lam, S. G. Mhaisalkara, and M. Srinivasan, *Energy Environ. Sci.* **4**, 413 (2011).
- ⁴W. Guo, X. Xue, S. Wang, C. Lin, and Z. Wang, *Nano Lett.* **12**, 2520 (2012).
- ⁵T. Chen, L. Qiu, Z. Yang, Z. Cai, J. Ren, H. Li, H. Lin, X. Sun, and H. Peng, *Angew. Chem. Int. Ed.* **51**, 11977 (2012).
- ⁶T. Song and B. Sun, *ChemSusChem* **6**, 408 (2013).
- ⁷Z. Zhang, X. Chen, P. Chen, G. Guan, L. Qiu, H. Lin, and H. Peng, *Adv. Mater.* **26**, 466 (2014).
- ⁸T. Miyasaka and T. N. Murakami, *Appl. Phys. Lett.* **85**, 3932 (2004).
- ⁹C. Lo, C. Li, and H. Jiang, *AIP Adv.* **1**, 042104 (2011).
- ¹⁰A. S. Westover, K. Share, R. Carter, A. P. Cohn, L. Oakes, and C. L. Pint, *Appl. Phys. Lett.* **104**, 213905 (2014).
- ¹¹A. Takshi, H. Yaghoubi, T. Tevi, and S. Bakhshi, *J. Power Sources* **275**, 621 (2015).
- ¹²X. Zhang, X. Huang, C. Li, and H. Jiang, *Adv. Mater.* **25**, 4093 (2013).
- ¹³X. Huang, X. Zhang, and H. Jiang, *J. Power Sources* **248**, 434 (2014).
- ¹⁴P. Wang, S. M. Zakeeruddin, J. E. Moser, M. K. Nazeeruddin, T. Sekiguchi, and M. Grätzel, *Nat. Mater.* **2**, 402 (2003).
- ¹⁵T. Stergiopoulos, I. M. Arabatzis, G. Katsaros, and P. Falaras, *Nano Lett.* **2**, 1259 (2002).
- ¹⁶J. H. Kim, M. S. Kang, Y. J. Kim, J. Won, N. G. Park, and Y. S. Kang, *Chem. Commun.* **2004**, 1662.
- ¹⁷J. H. Wu, S. C. Hao, Z. Lan, J. M. Lin, M. L. Huang, Y. F. Huang, L. Q. Fang, S. Yin, and T. Sato, *Adv. Funct. Mater.* **17**, 2645 (2007).
- ¹⁸Q. Li, J. Wu, Z. Tang, Y. Xiao, M. Huang, and J. Lin, *Electrochim. Acta* **55**, 2777 (2010).
- ¹⁹K. Fan, T. Peng, J. Chen, X. Zhang, and R. Li, *J. Mater. Chem.* **22**, 16121 (2012).
- ²⁰X. Zhang, X. Huang, and H. Jiang, *Phys. Chem. Chem. Phys.* **15**, 6864 (2013).
- ²¹Z.-S. Wang, H. Kawauchi, T. Kashima, and H. Arakawa, *Coord. Chem. Rev.* **248**, 1381 (2004).
- ²²A. Hagfeldt, G. Boschloo, L. Sun, L. Kloo, and H. Pettersson, *Chem. Rev.* **110**, 6595 (2010).
- ²³Y. Yang, C. H. Zhou, S. Xu, H. Hu, B. L. Chen, J. Zhang, S. J. Wu, W. Liu, and X. Z. Zhao, *J. Power Sources* **185**, 1492 (2008).